Fractal Analysis of Butanol/Gasoline Surrogate Blends Combustion in an Optical Direct-Injection Engine

Hongyu Wang, Zhe Sun, Xuesong Li, Min Xu*
School of Mechanical Engineering, Shanghai Jiao Tong University, Dongchuan Road 800 Shanghai, China 200240
*Corresponding author email: mxu@sjtu.edu.cn

Abstract
Fractal characteristics of the flame front surface and the internal flow field was experimentally observed during the propagation of the flame in the cylinder. The calculation and analysis of the flame fractal dimension based on the flame image are essential to understand the flame structure and assess its combustion quality. This paper established a fractal analysis method to predict flame characteristics. A gasoline direct injection (GDI) engine fuelled with the butanol isomer/gasoline surrogate blends of different proportions was used to get the flame images, and the box-counting method was used to calculate the fractal dimension of the flame edge in the image plane and the gray-scale intensity surface of the premixed flame region. The apparent flame speed and the area ratio of flame were calculated from the flame image and comprehensively analysed together with fractal dimension. Results showed that the addition of butanol to the gasoline surrogates makes flame propagation speed slower except TPRF-nB, and the flame propagating speed increases with a higher fractal dimension. However, the fractal dimension of the two-dimensional flame edge is unstable and unreliable due to its poor resistance against external disturbances. So, it is a better method to combine two-dimensional and three-dimensional fractal analysis, which could predict the flame speed more accurately.

Keywords
Fractal dimension; Butanol/Gasoline Surrogate Blends; Optical engine

Introduction

Gasoline direct injection (GDI) engines are increasingly used for its higher combustion efficiency and reduced fuel consumption. However, the increased PM emission caused by spray-wall interaction is difficult to control through any optimization of the engine. The utilization of alternative fuel like alcohol is widely studied and considered an effective method to enhance in-cylinder combustion and soot oxidation [1-2].

Among all kinds of alcohols, the blending fraction with gasoline and calorific value of butanol are higher compared to methanol and ethanol [3]. Butanol has four different isomers include n-butanol, iso-butanol, sec-butanol, and tert-butanol. For their blends with gasoline, the different molecular structure of isomers has a different influence on the combustion of butanol isomer and gasoline in the internal combustion engine. Chang et al. [4] confirmed the reduction of the fuel reactivity after the addition of butanol isomers, and Li et al. [5] reported that all butanol isomers increase flame speed and shorten the burning durations except tert-butanol. The concentration of active radicals such as H and OH which accelerates combustion increases with the addition of n-butanol [6]. And for SI engine experiments, Lattimore et al. [7] reported that the addition of n-butanol to gasoline advanced the CA50 and shortened the combustion duration. These studies concluded that flame speed and combustion duration changes with the addition of different kinds of butanol isomers.

For analyzing the flame structure of different butanol isomer/gasoline blends, the fractal dimension can be exploited as a measurement of geometric roughness and complexity of the flames [8-10]. Mandelbrot et al [11] began the application of fractal analysis to turbulence and

suggested that surfaces of constant properties of a passive scalar in turbulent flows possess fractal character. Many works of fractal analysis of flame have been conducted. Dobashi et al [12] reported that if the fractal dimension of a spherically-propagating premixed flame is known, then the flame area and hence the flame speed can be predicted. Molkov et al [13] found that the fractal sub-model that computes augmentation to flame propagation velocity using the fractal dimension can correctly predict the experimentally observed flame acceleration.
These studies have modelled a relationship between flame speed and fractal dimension of the flame front surface which was estimated through flame edge image. The fractal analysis of 2D flame edge could not completely reflect flame propagation especially along the direction of the camera lens. In this study, four butanol isomers (iso-butanol, n-butanol, sec-butanol, tert-butanol), as well as their 30 vol% blends with toluene primary reference fuel (TPRF), were tested through a GDI optical engine. Such effort includes flame visualization, flame parameter analysis, and fractal analysis of both planar contours of flame and the gray-level intensity surface in three-dimensional space.

Fractal Model of Turbulent Flames

The fractal characterization of the flame surface was modelled based on the relationship between the turbulence of combustion and scales of wrinkling of the flame surface which can be measured by the fractal dimension. Assuming homogeneous, isotropic turbulence and neglecting the influence on the turbulence of combustion, the ratio of the turbulent burning velocity (S_T) to the laminar burning velocity (S_L) can be expressed as [14-17]:

$$\frac{S_T}{S_L} = \left(\frac{l}{\eta}\right)^{D-2} = g\left(f A_t^{\frac{1}{4}} R_e^{\frac{3}{4}}\right)^{D-2} \quad (1)$$

where η and l are respectively the inner- and outer-cutoffs. Re is the Reynolds number of the flame and A_t is a constant of order one. D is the fractal dimension of the flame surface which needs to be calculated through flame images. For the final form of the fractal model, the g and f in equation 1 is the coefficient of flame stretch correction which was expressed as

$$g = 1 - \alpha C_k \left[(T_1+T_0)/2T_0\right]^{\frac{1}{2}} \times (A_t/15)^{1/2} \times (S'/S_L)^2 R_e^{-1/2} \quad (2)$$

$$f = 1 - (1 - A_t^{-1/4} R_e^{-3/4}) \times \exp(-A_t^{-1/4} R_e^{-3/4} S'/(u_0 g)) \quad (3)$$

where C_k is an empirical constant; T_1 and T_0 are respectively the adiabatic flame temperature and the reactant gas temperature; α is a constant related to the activation and adiabatic flame temperature of the combustion; S' refers to the root mean square of the turbulent velocity fluctuations.
The relationship between the flame speed and the fractal dimension of the flame surface is proposed through the model. Thus, the effect of flame stretch reduces the influence of fractal dimension on the turbulent flame speed, and the variety of the constants, A_t, Re and C_k may cause inaccuracy when comparing experimental results and model predictions.

Experimental Setup

Experiments were conducted in a four-stroke, single-cylinder, water-cooled, GDI optical engine to observe the combustion and flame propagation of different types of butanol isomers and gasoline surrogate blends. The structure and main components of the optical engine system are shown in **Figure 1**, and **Table 1** summarizes the specifications of engine and operation parameters. The engine was motored at a speed of 1000 rpm by an AVL AC dynamometer. The temperature boundary of the cylinder was controlled by a mental liner equipped with a circulating water jacket. An AVL coolant and lubricant oil supply conditioning

unit was utilized to keep the engine coolant and oil temperature at 60°C with an uncertainty of ±1°C. Through an electrical throttle valve, the intake manifold absolute pressure was regulated at 63 kPa, and the swirl ratio was controlled at 0.55. A symmetrical eight-hole fuel injector was installed at the top of the cylinder, and a spark plug was set next to it.

In this research, two hundred cycles were investigated and recorded through the optical engine system for each type of fuel. The in-cylinder pressure trace was acquired at a resolution of 0.1°CA under the measurement and analysis of a Kibox combustion analyser (2893A), a piezoelectric pressure transducer (Kistler 6125A), and a charge amplifier (Type 5064). The recorded pressure data were post-processed to calculate the indicated mean effective pressure (IMEP), and the nominal IMEP is 5.5 bar for all test conditions. The coefficients of cyclic variation of IMEP (COV) used to evaluate the combustion instability were below 3.2%. A computer is used to set these electronic control parameters and maintain the synchronization of these components through a synchronizer.

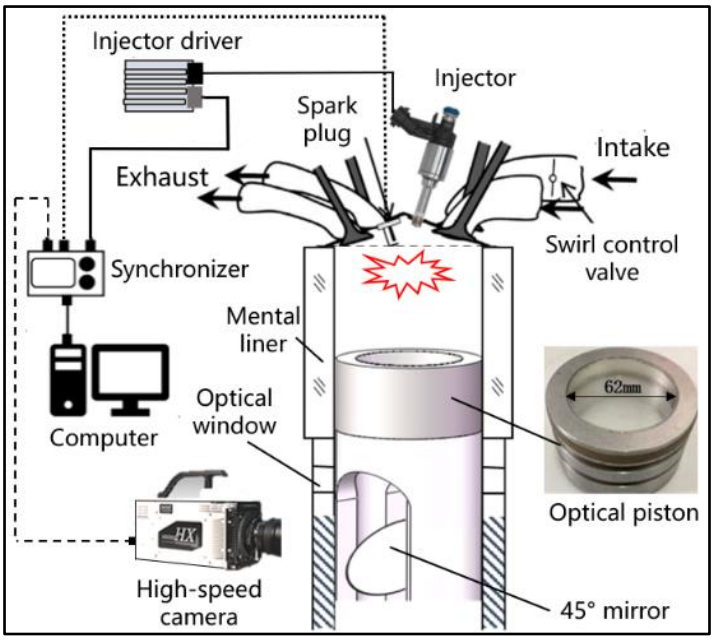

Figure 1. Layout of the optical engine system.

Table 1. Specifications of engine and operating conditions.

Engine Paramaters	Unit	Values
Bore	mm	86
Stroke	mm	94.6
Compression ratio	—	11:1
Speed	rpm	1000
Lubricant/coolant temperature	°C	60±1
Number of holes	—	6
Fuel injection pressure	MPa	10
Injection timing	°bTDC	270
Injection duration	μs	2450
Ignition timing	°bTDC	13
Ignition dwell	μs	1500
Swirl ratio	—	0.55
Intake manifold absolute pressure	kPa	63

It can also be seen in **Figure 1** that the optical access to the combustion chamber was achieved through a 45-degree mirror and a piston with a quartz window which has a diameter of 62 mm. A high-speed RGB camera (HX-5E, NAC) equipped with a Zeiss 50 mm f/1.4 lens was used. Images were recorded simultaneously after the ignition signal given and the image only shows the flame propagation within the accessible circular area. And the shooting frequency of the camera is 12 kHz, so the exposure time is 83.3 µs which correspond to 2 frame/°CA. The image taken has a spatial resolution of 547×607 pixels. The pixel bit depth of the camera was set to 12bit and black balance and white balance were validated. Under these conditions, 200 images were recorded from -13 to 87°aTDC in 230 consecutive cycles.

Image Processing

To analyse the digital information of flame images, the images recorded were first considered as the 2-dimensional projection of flame propagation. The processing procedure of flame images is shown in **Figure 2**. The application of an appropriate circular mask with a diameter of 210 pixels (**Figure 2** (a)) was first utilized to remove the spurious light including reflections and halo effects at the boundaries of the optical window. Considering the actual diameter of the optical window, which was 62mm, the conversion relation between image size and real size was 0.1746mm/pixel. After the enhancement of the image, a binarizing technique was performed to the remaining unmasked area while a proper threshold value was chosen depending on the balance between the integrity and elimination of image noise, then the flame and surrounded area were shown in white and black. **Figure 2** (e) shows the edge of flame which was extracted from the binarized image using “canny” edge detect operators, the flame boundary was outlined with a white line to clearly show the flame area. From the flame images, flame area, flame radius and apparent flame speed could be calculated. The flame area was regarded as the number of white pixels in the binarized image. The flame radius was calculated through a transition from the binarized image to an equivalent circle with an identical area to the flame [18]. The apparent flame was measured by dividing the different values of the flame radius by the time. The evaluation of the fractal dimension of the flame edge based on the edge image was conducted through the box-counting approach.

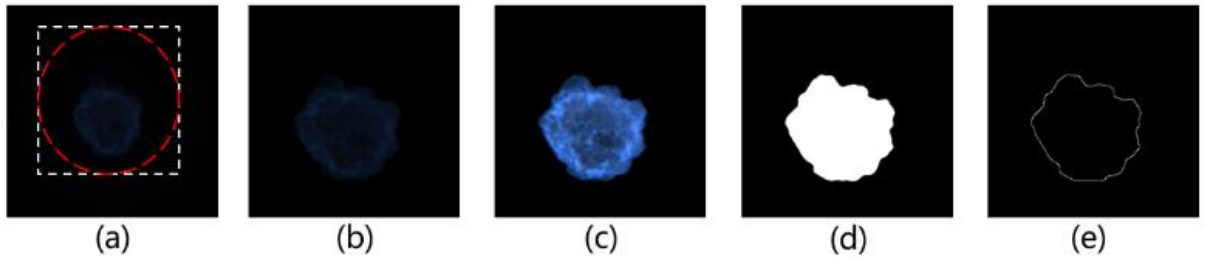

Figure 2. Sketch of flame image postprocessing (a) Raw image (b) Mask enabled image (c) Enhanced image (d) Binarized image (e) Flame edge.

For analysing the fractal characteristics of premixed turbulent flame, the gray-level intensity surface of the premixed flame region is obtained through the image processing procedure shown in **Figure 3**. After the application of the circular mask, the first step consists in the extraction of the premixed flame region from the RGB image. In this phase, the HSV colour model was applied to divide the image into portions corresponding to the premixed flame region, the diffusion region, and the near-infrared region. The premixed region is defined as a Hue degree range of 118~252° in the HSV colour model, so the image of the premixed flame region was isolated according to the specified Hue degree range after transforming from the RGB space to the HSV space using the command rgb2hsv in MATLAB. A transition was conducted from the false-colour 12-bit image (**Figure 3** (b)) to the 8-bit grey-level image (**Figure 3** (c)). Considering the gray-scale of each pixel as the value of z coordinate, the gray-

level intensity surface was obtained as is shown in **Figure 3** (d). The fractal dimension of the gray-level intensity surface was calculated by three-dimensional box-counting method.

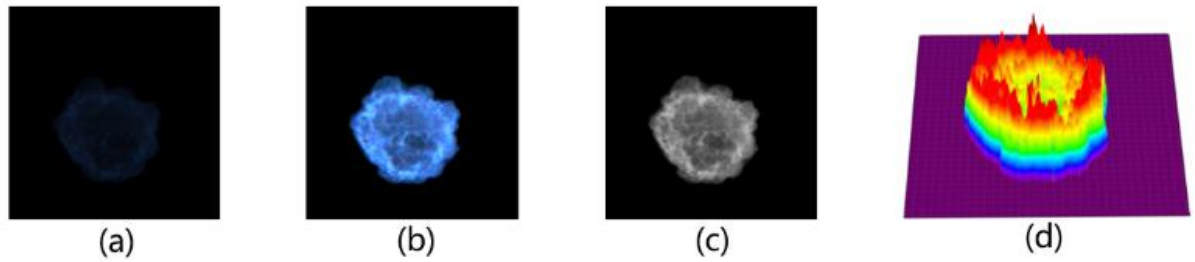

Figure 3. Procedure to obtain gray-level intensity surface of the premixed flame region (a) Mask enabled image (b) premixed flame region (c) gray-scale image (d) gray-level intensity surface.

Methodology of Fractal Analysis

Many approaches which can be used to estimate fractal dimension were discussed by Michael [19]. Among them, the box-counting method has been widely used in fractal dimension calculating for its simplicity and accuracy in algorithmic expression and has also been proved useful for flames especially when the turbulent intensity is high [20]. In n-dimensional Euclidean space, box-counting based fractal dimension of a bounded fractal set is defined as

$$D=\frac{log(N_r)}{log(1/r)} \tag{4}$$

where N_r is the minimum number of boxes at size r that are required to cover the bounded fractal set which can be chaotic curves in a plane or an irregular surface in three-dimensional space. Due to the non-ideal characteristics of flame as a fractal set, the box-counting approach can approximate the fractal dimension of the flame front surface through the processed flame image.

The image of the flame edge is considered as the projection of the flame surface along the direction of the cylinder [21]. Then the fractal dimension of the edge image can be calculated using the box-counting method shown as graphical demonstration in **Figure 4**. The greyed boxes in the mesh grid are those which contain the contour line. For different box size of r, the number of these boxes is counted and recorded as the N_r [22].

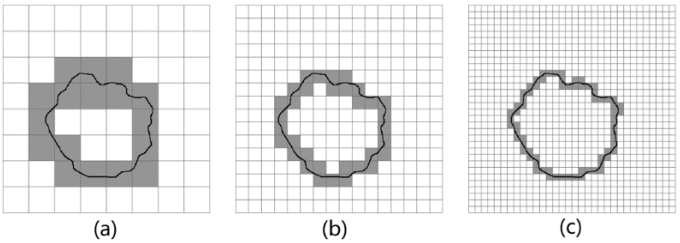

Figure 4. Graphical demonstration of the box-counting method with box scale of (a) 32 pixels (b) 16 pixels (c) 8 pixels.

Besides, for analyzsing the 3D fractal characteristic of flame, the flame propagation in the direction of the piston needs to be considered. The gray-level value is utilized to evaluate the intensity of flame propagation along the axes in the cylinder. The fractal dimension of the gray-scale image is estimated through 3D box-counting approach shown in **Figure 5**. The XY-plane presents the image plane which is partitioned into grids of size r×r pixels. By the way, z coordinate denotes the intensity value of the gray-scale image [23]. The total number of boxes that cover the rough surface of the gray-scale image can be calculated and recorded corresponding to the box size r.

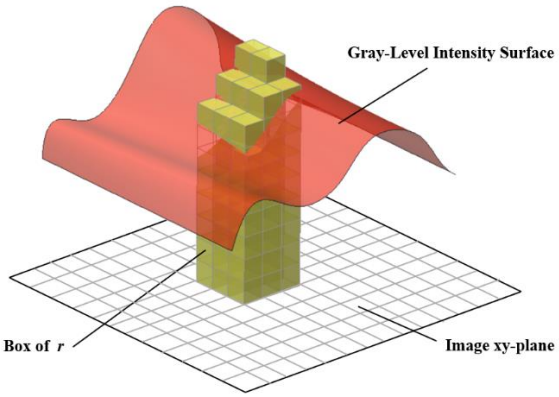

Figure 5. Sketch for the determination of boxes in a three-dimensional surface.

For both the flame edge and the gray-level intensity surface of the flame image, analysis of the number of boxes versus the box size curve gives the fractal dimension. **Figure 6** shows the curve of the recorded data, which shows a significant linear relationship between log(N_r) and log(1/r), and the estimate of the fractal dimension is the slope of this graph [20].

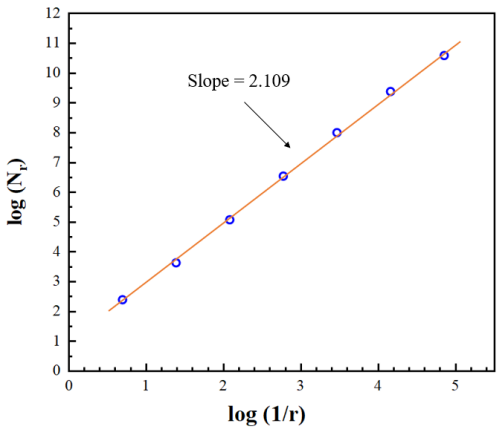

Figure 6. Curve of log(N_r)–log(r) relation.

Results and Discussion

Flame Analysis

The flame propagation for five kinds of butanol isomers and TPRF surrogate blends is illustrated in **figure 7**. The range of flame images, which are denoised and enhanced to achieve a better visualization, were selected from -10 to 10 °CA aTDC to exhibit the structure evolution from early ignition to CA10 of combustion. The flame analysis includes colour intensity distribution and the edge shape of the flame image. At the crank angle of -10 °CA, the images show the initiation of the flame core after ignition at -13 °CA aTDC. The flame is to propagate from the flame core to the cylinder wall, so the time flame core appears is the start of flame propagation. At this point, flame cores of TPRF, TPRF-nB, TPRF-iB, TPRF-sB have appeared and the flames have developed for a while, while TPRF-tB flame has just initiated. Furthermore, for the whole propagation process, the flame edge scale of TPRF-nB is larger than the other four fuels which means the flame of TPRF-nB develops at the fastest speed in the five butanol isomers and TPRF surrogate blends.

The flame images in **Figure 7** also show some difference of colour distribution among different test fuels. This flame colour of TPRF-nB is purplish-blue which means the Hue degree range of TPRF-nB flame is wider and this causes a more complicated premixed flame region and a rougher gray-level intensity surface. Also, more yellow spots visually noted in the flame images

of the butanol/gasoline surrogate blends. This might result from poor fuel atomization of butanol blends which generates more fuel droplets that cause local diffusive combustion[24].

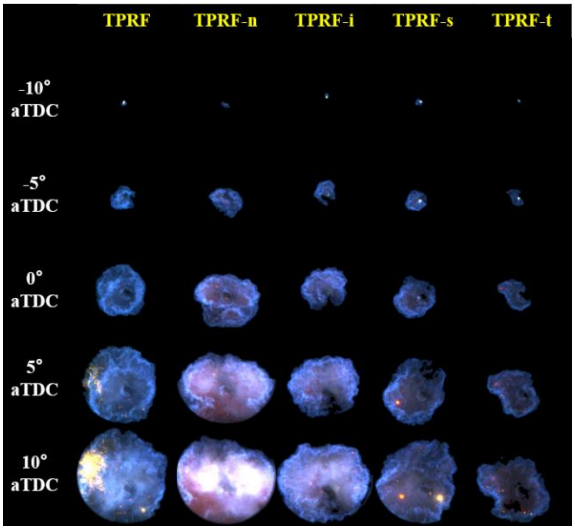

Figure 7. Flame development of TPRF/butanol isomers blends.

The apparent flame speed and flame area ratio are illustrated in Figure 8. As the analysis result from the flame propagation images, TPRF-nB shows the highest apparent flame speed compared to the pure TPRF and three other butanol/gasoline surrogate blends especially in the range of -7 to 0 °CA aTDC. The apparent flame speed of five tested fuels shows the order of TPRF-nB > TPRF > TPRF-iB > TPRF-sB > TPRF-tB. The result among different butanol/gasoline surrogate blends is expected to the effect of n-heptane concentration. The flame speed improves as the n-heptane increases [24]. The addition of n-butanol to TPRF improves the flame propagating speed in the first half of the flame expansion stage. The negative influence of tert-butanol to the flame propagating speed is the most serious and the large fluctuation in the range of 5 to 7 °CA aTDC might result from instability of combustion. A sudden increase of apparent flame speed at the point of around -8 °CA aTDC is also shown in **Figure 8** (a), which locates at the conversion point from flame core generation to flame propagation.

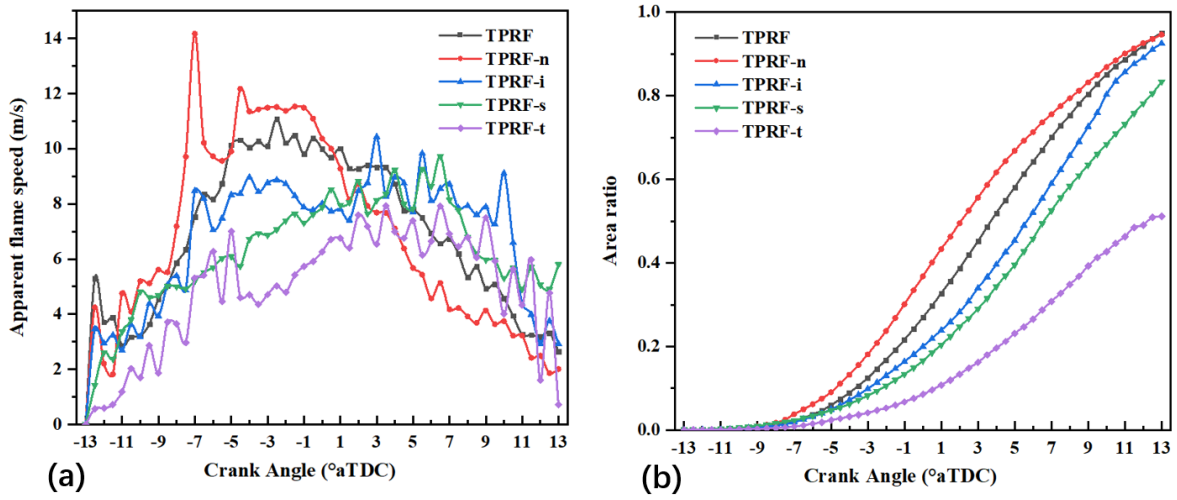

Figure 8. Parameter variation in the flame propagation: (a) apparent flame speed, and (b) flame area ratio

Figure 6 (b) shows the area ratio variation in the propagating process of flame. The maximum radius is 31 mm because of the limitation of the optical access window, and the maximum flame area is unity for each circle when the flame reaches this limit. The area ratio is calculated by the flame area divided by the maximum area. The order of the area ratio at different crank angles is TPRF-nB > TPRF > TPRF-iB > TPRF-sB > TPRF-tB, which shows the same order as apparent flame speed. Curves of apparent flame speed in **Figure 8** (a) also represent the variation of the slope of area ratio curves in **Figure 8** (b). With the decreasing of TPRF-nB flame speed in the late stage of flame development, the increasing speed of area ratio of TPRF-nB also decreases and gets close to the area ratio of TPRF.

Fractal Analysis

Some of the calculating results of the fractal dimension of five kinds of butanol isomers and TPRF surrogate blends is shown in **Figure 9**. The crank angle for estimating the fractal dimension of the flame edge in the image plane is selected at -5 °CA aTDC. As shown in **Figure 9** (a), the image was trimmed from the original flame edge image to obtain a better visualization without changing the relative size. The order of the two-dimensional fractal dimension of five test fuel is TPRF-iB > TPRF > TPRF-sB > TPRF-tB > TPRF-nB at -5 °CA aTDC. The flame area and the edge length of the TPRF-nB flame are larger than the other four test fuels. However, the Fractal dimension of the TPRF-nB flame edge is the lowest. This results from the less roughness of the TPRF-nB flame edge and the shape is more regular than the other four test fuels. Moreover, an obvious breach was noted in the lower right of TPRF-iB flame, which is due to the covering of the ignition plug. This might cause mistakes of the fractal dimension of the flame edge in the early state of flame development.

Figure 9 (b) shows the calculating result of the gray-level intensity surface at the point of 1 °CA aTDC. The image below the image premixed flame region is the corresponding gray-level intensity surface. Most of the fractal dimensions are in the range of 2 to 3, for the surface is considered as the geometry between a plane and a body. The order of the three-dimensional fractal dimension of five test fuel is the same as that of apparent flame speed, which is TPRF-nB > TPRF > TPRF-iB > TPRF-sB > TPRF-tB. The three-dimensional fractal dimension of TPRF-nB gray-level intensity surface which has more raised parts and higher peaks than other surfaces and more surface fluctuation.

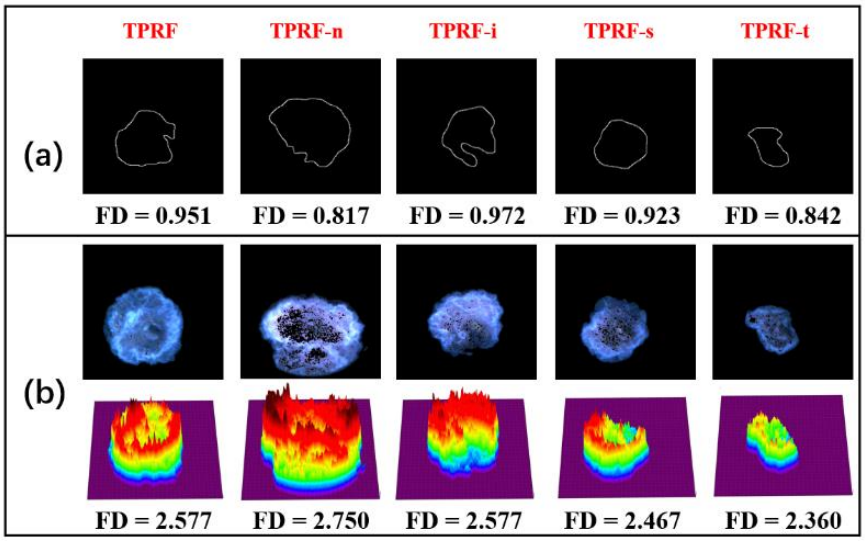

Figure 10. Calculating results of fractal dimension: (a) FD of flame edge at -5 °CA aTDC (b) FD of gray-level intensity surface at 1 °CA aTDC

The change of fractal dimension of flame front with crank angle for five test fuels is illustrated in **Figure 10**. A steep increase is seen after the start of ignition in **Figure 10** (a), which shows the flame edge in the image plane. This corresponds to the period of generation of the flame core. Clear order of five test fuels can be noted at the range of -11 to -5 °CA aTDC, however, the curves of five test fuels after -5 °CA are intertwined without any regulation. The reason for such observation is expected to two crucial aspects. For the calculating method of fractal dimension, the number of boxes covering the edge line is obvious few, which leads to more subtle differences among different test fuels. Also, the covering of the ignition plug leads to the appearance of breaches in the flame edge image, which increases the roughness of the flame edge, and the result of fractal dimension deviates from the true values. On the other hand, the average fractal dimensions from -13 to 13 °CA aTDC of five test fuels was calculated, which are 0.845, 0.894, 0.857, 0.847 ,0.834 for TPRF, TPRF-nB, TPRF-iB, TPRF-sB, TPRF-tB. This result is found to has the same order as that of apparent flame speed.

The fractal dimension of the gray-level intensity surface of the premixed flame region presented in **Figure 10** (b) shows a more regular result. In the range from -12 to -6 °CA aTDC, curves of five test fuels are almost overlapped at the fractal dimension level of around 2.1. After the flame begins to propagating, the three-dimensional fractal dimension of five fuels separate and the order is TPRF-nB > TPRF-iB > TPRF > TPRF-sB > TPRF-tB, which is the same as that of apparent flame speed except for the order of TPRF-iB and TPRF. This might be due to tiny raise parts of the gray-level intensity surface of the TPRF-iB flame caused in the process of extracting the premixed flame region.

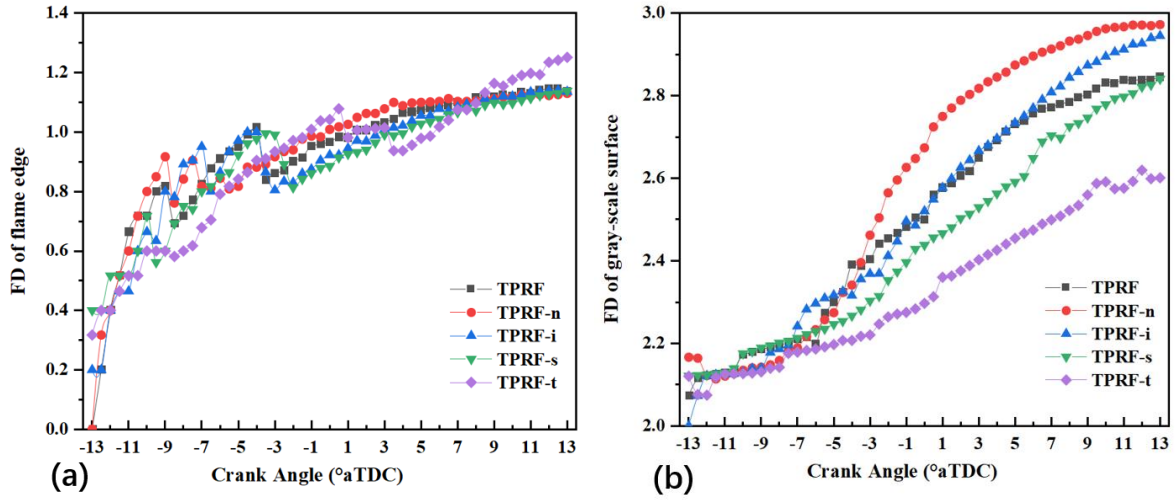

Figure 10. Fractal dimension of (a) flame edge in the image plane (b)gray-level intensity surface of the premixed flame region

Conclusions

In this paper, the flame propagation behaviours and fractal dimension of the flame front of five kinds of butanol isomer/gasoline surrogate blends were studied. The mix proportion of blends is 30 vol% butanol isomers and 70 vol% TPRF gasoline surrogates. Experiments and analysis show that different kinds of butanol have a different impact on the combustion performance of gasoline, and the result of fractal analysis has a closed link with flame propagating speed. Detailed conclusions are listed as follows:

1. Addition of butanol to the gasoline surrogates makes flame propagation speed slower except TPRF-nB. The reasons include the slower mixing process and larger dual droplets produced by butanol addition. The positive influence of TPRF-nB results from chemical

reasons for its purplish-blue flame which differs from other kinds of butanol isomer and gasoline surrogate blends.
2. The scale of the fractal dimension of flame front can reflect the wrinkle rating and roughness of flame, which is related to the turbulence intensity and turbulent velocity of flame. The flame propagating speed increases with a higher fractal dimension.
3. Fractal dimension of the flame edge in the image plane is less unstable and unreliable due to its poor resistance against external disturbances such as the covering effect of ignition plug, and the number of boxes counted in the calculating process is relatively few, the real difference on fractal dimension among different conditions could be easily covered by deviation especially in produced in the image processing. The combination of two-dimensional and three-dimensional fractal analysis could be a better method to predict the flame speed more accurately.

References

[1] Zheng X, Zhang S, Wu Y, Xu G, Hu J, He L, et al. Measurement of particulate polycyclic aromatic hydrocarbon emissions from gasoline light-duty passenger vehicles. J Clean Prod, 2018. 185: p.797–804.

[2] Qian Y, Li Z, Yu L, Wang X, Lu X. Review of the state-of-the-art of particulate matter emissions from modern gasoline fueled engines. Applied Energy, 2019. 238: 1269–98.

[3] Jin C, Yao M, Liu H, Lee CFF, Ji J. Progress in the production and application of n-butanol as a biofuel. Renew Sustain Energy Rev 2011. 15: 4080–106.

[4] Chang Y, Jia M, Xiao J, Li Y, Fan W, Xie M. Construction of a skeletal mechanism for butanol isomers based on the decoupling methodology. Energy Convers Manag, 2016. 128: 250–60.

[5] Li L, Wang T, Duan J, Sun K. Impact of butanol isomers and EGR on the combustion characteristics and emissions of a SIDI engine at various injection timings. Appl Therm Eng, 2019. 151: 417–30.

[6] Li X, Hu E, Meng X, Lu X, Huang Z. High-temperature oxidation kinetics of iso-octane/n-butanol blends-air mixture. Energy, 2017. 133: 443–54.

[7] Lattimore T, Herreros JM, Xu H, Shuai S. Investigation of compression ratio and fuel effect on combustion and PM emissions in a DISI engine. Fuel, 2016. 169:68–78.

[8] Chatakonda, O. , Hawkes, E. R. , Aspden, A. J. , Kerstein, A. R. , Kolla, H. , & Chen, J. H. . On the fractal characteristics of low damkoehler number flames. Combustion & Flame, 2013. 160(11), 2422-2433.

[9] Yang Yi, Luo Geng, Guo Jing. Experimental study on the fractal characteristic of methane explosion flame. Safety Science, 2012. 50(4): p. 679-683.

[10] Denet B . Fractal Dimension of Turbulent Premixed Flames for Different Turbulence Spectra. Combustion Science and Technology, 2000, 159: p.305-314.

[11] B.B. Mandelbrot, J. Fluid Mech. 72 (1975) 401–416.

[12] Dobashi, R., Kawamura, S., Kuwana, K., & Nakayama, Y. Consequence analysis of blast wave from accidental gas explosions. Proceedings of the Combustion Institute, 2011. 33, 2295e2301.

[13] Molkov, V., Makarov, D., & Schneider, H. LES modelling of an unconfined large-scale hydrogen-air deflagration. Journal of Physics D, 2006. 39, 4366e4376.

[14] Gouldin, F. C.. An application of fractals to modeling premixed turbulent flames. Combustion & Flame, 1987. 68.3: p.249-266.

[15] INAGE, Shin-ichi, KOBAYASHI, Hironobu, KOBAYASHI, & Nariyoshi. A theoretical evaluation of fractal dimension of turbulent flame. Jsme International Journal.ser.b Fluids & Thermal Engineering, 1999.

[16] Dae Hoon Lee & Sejin Kwon. Statistical analysis of the fractal nature of turbulent premixed flames, Combustion Science and Technology, 2003. 175:7, 1317-1332

[17] Yung-Cheng Chen, Mohy S. Mansour. Geometric interpretation of fractal parameters measured in turbulent premixed Bunsen flames. Experimental Thermal and Fluid Science, 2003. 27(4): p.409-416.

[18] Gu X, Huang Z, Wu S, Li Q. Laminar burning velocities and flame instabilities of butanol isomers-air mixtures. Combust Flame, 2010. 157: 2318–25.

[19] Frame, Michael，Urry, Amelia, Fractal worlds: grown, built, and imagined, 2016.

[20] N. Sarkar, B.B. Chaudhuri, an efficient differential box-counting approach to compute fractal dimension of image, IEEE Trans. Syst. Man Cybern, 1994. 24 (1) p. 115–120.

[21] Daniel Sawicki, Zbigniew Omiotek, Evaluation of the possibility of using fractal analysis to study the flame in the co-firing process, Proc. SPIE 10808, Photonics Applications in Astronomy, Communications, Industry, and High-Energy Physics Experiments, 2018. 108081G

[22] Chatakonda O , Hawkes E R , Aspden A J , et al. On the fractal characteristics of low Damkoehler number flames. Combustion & Flame, 2013. 160(11): 2422-2433.

[23] Panigrahy, C., Seal, A, Mahato, NK, quantitative texture measurement of gray-scale images: Fractal dimension using an improved differential box counting method, Measurement, 2019. 147.

[24] Zhe, S. A. , Mc, A. , Mna, B. , Xl, A. , Dha, C. , & Min, X. A. . Study of flash boiling combustion with different fuel injection timings in an optical engine using digital image processing diagnostics. Fuel, 284.

[25] Liao YH, Roberts WL. Laminar Flame Speeds of Gasoline Surrogates Measured with the Flat Flame Method. Energy and Fuels, 2016. 30: 1317–24.